Proceedings of the ASME 2019 International Design Engineering Technical Conferences & Computers and Information in Engineering Conference
IDETC/CIE 2019
August 18-21, 2019, Anaheim, CA, USA

IDETC2019-97665

A MODULAR APPROACH TO LEVEL CURVE TRACKING WITH TWO NONHOLONOMIC MOBILE ROBOTS

Sarthak Chatterjee
Department of Electrical, Computer, and Systems Engineering
Rensselaer Polytechnic Institute
Troy, New York, 12180
Email: chatts3@rpi.edu

Wencen Wu*
Department of Computer Engineering
San Jose State University
San Jose, California, 95192
Email: wencen.wu@sjsu.edu

ABSTRACT

In this paper, we consider the problem of tracking noisy two-dimensional level curves using only the instantaneous measurements of the field, taken by two mobile agents, without the need of estimating the field gradient. To do this, we propose a dual-control-module structure consisting of the formation control and curve tracking modules. The former uses the linear velocity of the agents to generate the angular velocities, which are then used to maintain a constant distance between the two agents. The latter uses the instantaneous field measurements to generate the linear velocities of the two agents to successfully track level curves. The modular approach decouples the problems of formation control and curve tracking, thus allowing the seamless design of the two modules. We show that the proposed dual-module control structure allows fast and accurate tracking of planar level curves.

INTRODUCTION

The past couple of years have seen an increasing use of mobile sensor networks that have been used to collect information that is utilized for dynamic tracking of physical properties of the surrounding environment. They are a reliable and highly cost-effective means to monitor environmental changes for extended periods of time. Relatively few numbers of mobile sensor networks may be used very efficiently to explore complex, expansive, and remote environments, allowing applications in motion monitoring, sensor network platforms, and data dissemination and collection. [1–4] are a few works in this regard.

In recent years, the works in [5–8] have investigated the problem of exploration of environmental boundaries. More specifically, the approach in [9] dealt with the problem of large-scale level curve tracking of noisy environmental scalar fields by using multiple motile sensor platforms. Further, the work in [10] builds on the above idea to develop a scheme to track three-dimensional level curves by using filtering strategies to estimate the field value at the formation center and using Taubin's algorithm [11] to estimate curvatures of the field lines.

Research has also been done in the area of gradient-free tracking of planar level curves [12–21]. We generally have no information about the field gradient, and estimating it is also difficult because we need simultaneous knowledge of the field values at multiple locations. Using a minimum number of mobile sensors that have access to only the instantaneous values of the field is therefore an attractive proposition.

In this paper, we propose a gradient-free modular approach to the tracking of level curves in noisy scalar fields using two unicycles. In doing so, we show how to achieve fast rates of convergence to the desired level curve using no gradient information and minimum computational power. We propose a dual-control-module structure that decomposes formation control and curve tracking as two different modules along the lines of [22]. In the formation control module, the angular velocities of the two mobile robots are designed so as to maintain a

*Address all correspondence to this author. The research work is supported by NSF grants CPS-1446461, CMMI-1663073, and CMMI-1917300.

fixed distance between them. In the curve tracking module, we use the instantaneous values of the scalar field to develop a hybrid controller that allows us to track noisy level curves without explicitly estimating the field gradient. The benefits of using such a dual-control-module structure are that the problem of designing the linear and angular velocities are decoupled. While the angular velocities deal only with formation control, the linear speeds deal with the fast gradient-free tracking of noisy two-dimensional level curves. We demonstrate two principal theoretical results.

The rest of the paper is organized as follows. We first talk about the curve-tracking problem and its formulation. Then, we perform a detailed analysis of the formation control module and derive conditions for the closed loop stability and input-to-state stability of the formation control dynamics. Finally, we introduce the control law which we use in the curve tracking module, and perform a detailed mathematical analysis of the stability and convergence of the two-agent system to the desired level value. We then present our simulation results and concluding remarks.

PROBLEM FORMULATION

We consider $z(\mathbf{r}) : \mathbb{R}^2 \to \mathbb{R}$ as a scalar field in a two-dimensional space, where $\mathbf{r} \in \mathbb{R}^2$ is the location. Every location of the field corresponds to a scalar value of a physical quantity such as light intensity, temperature or chemical concentration. We have the following assumptions on the field:

Assumption 1. 1. The field $z(\mathbf{r})$ is smooth with bounded values, that is, $z_{\min} \leq z(\mathbf{r}) \leq z_{\max}$, where $z_{\min}, z_{\max} > 0$.
2. The gradient $\left\|\nabla z(\mathbf{r})\right\| \neq 0$ and is bounded, i.e., $\rho_1 \leq \left\|\nabla z(\mathbf{r})\right\| \leq \rho_2$, where $\rho_1, \rho_2 > 0$.

Suppose $\gamma(\cdot)$ represents a simple, planar, closed, and regular curve in the field, parameterized using its arc length s. $s = 0$ defines the *starting point* for this curve, which we denote using the point $\mathbf{q}_0(s)$. The Frenet-Serret frame [23] in two dimensions, $(\mathbf{y}_0(s), \mathbf{x}_0(s))$ is such that we have $\mathbf{x}_0(s)$ as the unit tangent vector to the curve and $\mathbf{y}_0(s)$ as the unit normal vector to the curve. Let $\kappa(s)$ be the curvature of the curve such that $\kappa(s_0)$ gives the curvature of the curve at $s = s_0$. In such a scenario, the Frenet-Serret equations give the relationship between the frame $(\mathbf{y}_0(s), \mathbf{x}_0(s))$ and the kinematic properties of the curve as

$$\frac{\mathrm{d}\mathbf{x}_0(s)}{\mathrm{d}s} = -\kappa(s)\mathbf{y}_0(s), \tag{1a}$$

$$\frac{\mathrm{d}\mathbf{y}_0(s)}{\mathrm{d}s} = \kappa(s)\mathbf{x}_0(s). \tag{1b}$$

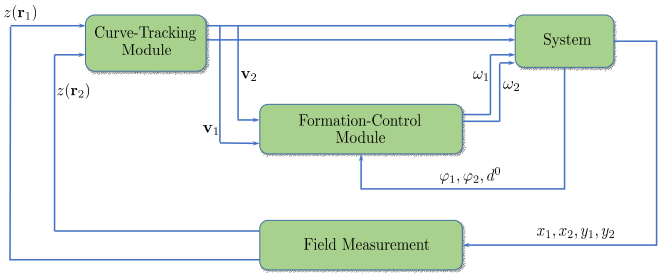

FIGURE 1. Schema for the dual-module curve-tracking approach proposed in the paper.

γ_0 is called a *level curve* of a function z if $z(\gamma_0(\cdot))$ is a constant function of s. Throughout this paper, we assume $\kappa > 0$, which implies that the tangent vector $\mathbf{x}_0$ is moving clockwise.

We consider the problem of estimating the boundaries of the field given by a particular level value by deploying two mobile robots in the field. The kinematics of the two robots are given as follows:

$$\dot{x}_i = v_i \cos\theta_i, \tag{2a}$$

$$\dot{y}_i = v_i \sin\theta_i, \tag{2b}$$

$$\dot{\theta}_i = \omega_i, \tag{2c}$$

for $i = 1, 2$. (x_i, y_i) are the coordinates of the rotation center of the i-th robot in the inertia frame, θ_i is the orientation angle, and v_i and ω_i are the linear and angular velocities respectively of the i-th mobile robot. We also assume that a 'no-slip' condition is imposed on the wheels of each mobile robot, so that the mobile robot cannot move sideways. This is a non-holonomic constraint. We also define $\mathbf{r}_1$ and $\mathbf{r}_2$ to be the coordinates of the rotation center of the two mobile robots. Also, let $\mathbf{v}_1$ and $\mathbf{v}_2$ denote the velocities of the two mobile agents. We relate $\mathbf{r}_1, \mathbf{r}_2$ to the coordinates (x_i, y_i) defined in equation (2) as follows: $\mathbf{r}_1 = \begin{bmatrix} x_1 \\ y_1 \end{bmatrix}, \mathbf{r}_2 = \begin{bmatrix} x_2 \\ y_2 \end{bmatrix}$. The mobile sensing agents are capable of taking measurements of the field at their current locations. If we define $y(\mathbf{r}_i)$, $i = 1, 2$ as the field value measured by the mobile robot i at its own rotation center, then the measurement process can be written as:

$$y(\mathbf{r}_i) = z(\mathbf{r}_i) + w(\mathbf{r}_i), \tag{3}$$

for $i = 1,2$. $w(\mathbf{r}_i)$ is assumed to be zero-mean white Gaussian noise arising from the noisy measurements or from the drifting level values of the field itself. We also assume that each mobile agent has access to the measurements and relative positions of the other agent. The measurements can be exchanged through wireless communication, and the relative locations of other agents can be obtained through cameras, lasers, sonar, etc. Denote the formation center of the agents by $\mathbf{r}_c$, where $\mathbf{r}_c = \frac{1}{2}\sum_{i=1}^{2}\mathbf{r}_i$. The velocity at the formation center $\mathbf{v}_c$ is given by $\mathbf{v}_c = \frac{1}{2}\sum_{i=1}^{2}\mathbf{v}_i$.

The fundamental problem we are looking to solve in this paper is as follows:

Problem 1: Consider the motion of the formation center $\mathbf{r}_c$ and the following assumptions:

1. There exists a unique level curve $\gamma_0(s)$ passing through $\mathbf{r}_c$ along the trajectory of $\mathbf{r}_c$.
2. The curvature $\kappa(s)$ of the level curve $\gamma_0(s)$ is bounded at every point of the trajectory of $\mathbf{r}_c$.

Given a desired level value z_d, design the linear and angular velocities of the two mobile robots such that the following two objectives are met:

1. *Formation Control:* The separation between the robots is maintained at a constant distance of d^0.
2. *Curve Tracking:* The moving direction of the formation center is aligned with the tangent direction of the desired level curve and the formation center converges to the level curve with value z_d, moving along the curve $\gamma_0(s)$. In other words, design $\mathbf{v}_1$ and $\mathbf{v}_2$, such that $z(\mathbf{r}_c) \to z_d$ as time $t \to \infty$.

We aim to design the control strategy without estimating the field gradient to reduce the computational cost and the sensitivity to noisy measurements. Furthermore, the control strategy should allow the center of the formation to achieve a fast rate of convergence to the level curve. In other words, the formation center converges to a small neighborhood of a desired level curve in finite time, which should be as short as possible.

For any physical wheeled robot, there is a limit to the maximum moving velocity it can have. Further, we must have smooth velocity input commands to the physical system to allow the low-level controller to track the velocity commands with sufficient accuracy. We therefore have the following assumptions on the control inputs v_i and ω_i:

Assumption 2. 1. For $i = 1,2$, $|v_i| \le v_{\max}$ and $|\omega_i| \le \omega_{\max}$, where $v_{\max} > 0$ and $\omega_{\max} > 0$ are the maximum allowable values of the linear and angular velocities of the agents respectively.
2. v_i and ω_i are sufficiently smooth.

Since, in the desired formation, $\omega_1 = \omega_2 = \frac{v_1 - v_2}{2}$, we also assume $\omega_{\max} > \frac{v_{\max}}{d^0}$ so that we can design the angular velocities for any $v_i > 0$ without the problem of saturation.

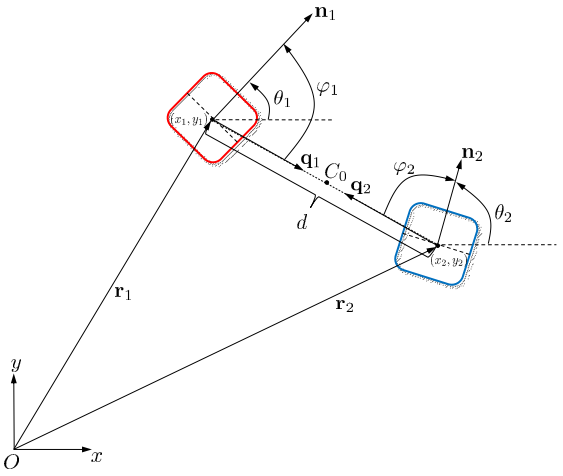

FIGURE 2. Schematic figure of the two unicycles and associated variables.

This paper proposes a two-module control strategy for the efficient tracking of two-dimensional planar level curves. The purpose of this dual-control-module structure is that it decouples the problem of formation control and curve tracking into separate modules, and gives us a streamlined solution of the problem. The formation control module uses the linear velocities of the two agents to design the angular velocities that keep the two-agent system in formation, that is, at a constant known distance from each other. The curve-tracking module on the other hand, uses only the instantaneous field values to design the linear velocities of the agents. This decoupling ensures that the angular velocities are used exclusively for formation control, and the linear velocities are used for level curve tracking. The following sections introduce the two modules in greater depth.

FORMATION-CONTROL MODULE

The formation control module takes in the linear velocities of the two robots, $\mathbf{v}_1$ and $\mathbf{v}_2$, as inputs and generates the angular velocities ω_1 and ω_2 as outputs. The desired formation as seen from Fig. 2 has $d = d^0$, $\varphi_1 = \pi/2$ and $\varphi_2 = -\pi/2$. This formation is where the two robots move in parallel with a constant distance of d^0 between them, regardless of their individual velocities.

The dynamics of the variables d, φ_1, and φ_2 are given by:

$$\begin{aligned} \dot{d} &= -v_1\cos\varphi_1 - v_2\cos\varphi_2, \\ \dot{\varphi}_1 &= \frac{v_1\sin\varphi_1 + v_2\sin\varphi_2}{d} + \omega_1, \\ \dot{\varphi}_2 &= \frac{v_1\sin\varphi_1 + v_2\sin\varphi_2}{d} + \omega_2. \end{aligned} \tag{4}$$

where $v_1 = \|\mathbf{v}_1\|$, $v_2 = \|\mathbf{v}_2\|$. To design a backstepping controller, define the tracking error variables

$$\begin{aligned}\mathscr{D}_d &= d - d^0,\\ \mathscr{D}_1 &= \cos\varphi_1 - \tfrac{k_d}{2}\left(d - d^0\right),\\ \mathscr{D}_2 &= \cos\varphi_2 - \tfrac{k_d}{2}\left(d - d^0\right),\end{aligned} \tag{5}$$

where $k_d > 0$ is a positive gain. Following the same approach used in [22], we take derivatives of (5), keeping in mind (4), to obtain:

$$\begin{aligned}\dot{\mathscr{D}}_d &= -k_d\left(\tfrac{v_1+v_2}{2}\right)\mathscr{D}_d - v_1\mathscr{D}_1 - v_2\mathscr{D}_2,\\ \dot{\mathscr{D}}_1 &= -\sin\varphi_1\left(\tfrac{v_1\sin\varphi_1+v_2\sin\varphi_2}{d} + \omega_1\right) + \tfrac{k_d}{2}\left(v_1\cos\varphi_1 + v_2\cos\varphi_2\right),\\ \dot{\mathscr{D}}_2 &= -\sin\varphi_2\left(\tfrac{v_1\sin\varphi_1+v_2\sin\varphi_2}{d} + \omega_2\right) + \tfrac{k_d}{2}\left(v_1\cos\varphi_1 + v_2\cos\varphi_2\right).\end{aligned} \tag{6}$$

Choosing

$$\begin{aligned}\omega_1 &= \tfrac{k_d}{2\sin\varphi_1}\left(v_1\cos\varphi_1 + v_2\cos\varphi_2\right) - \tfrac{v_1\sin\varphi_1+v_2\sin\varphi_2}{d} + k_{\mathscr{D}_1}\mathscr{D}_1,\\ \omega_2 &= \tfrac{k_d}{2\sin\varphi_2}\left(v_1\cos\varphi_1 + v_2\cos\varphi_2\right) - \tfrac{v_1\sin\varphi_1+v_2\sin\varphi_2}{d} + k_{\mathscr{D}_2}\mathscr{D}_2,\end{aligned} \tag{7}$$

where $k_{\mathscr{D}_1}, k_{\mathscr{D}_2} > 0$ gives us the closed-loop dynamics

$$\begin{bmatrix}\dot{\mathscr{D}}_d\\ \dot{\mathscr{D}}_1\\ \dot{\mathscr{D}}_2\end{bmatrix} = \underbrace{\begin{bmatrix}-k_d\frac{v_1+v_2}{2} & -v_1 & -v_2\\ 0 & -k_{\mathscr{D}_1} & 0\\ 0 & 0 & -k_{\mathscr{D}_2}\end{bmatrix}}_{\mathscr{A}}\begin{bmatrix}\mathscr{D}_d\\ \mathscr{D}_1\\ \mathscr{D}_2\end{bmatrix}. \tag{8}$$

We then introduce the following proposition, which is the main result of this section:

Proposition 1. *The closed-loop linear dynamics* (8) *is globally exponentially stable if* $(v_1+v_2) \geq 2\nu$ *where* $\nu > 0$ *is an arbitrarily small positive quantity.*

Proof. The matrix $\mathscr{A}$ as defined above is upper-triangular. We use a well-known result from linear algebra which states that the eigenvalues of a square upper-triangular matrix are the entries on its principal diagonal. Since $k_{\mathscr{D}_1}$ and $k_{\mathscr{D}_2}$ are defined to be positive, if $\frac{v_1+v_2}{2} \geq \nu$, $\nu > 0$, the eigenvalues of $\mathscr{A}$ are all negative. Since the system is linear, the stability property is also global. This proves our proposition. ■

We have shown that the system (8) is globally exponentially stable within a small neighborhood of the configuration $d = d^0$, $\varphi_1 = \pi/2$, and $\varphi_2 = -\pi/2$, or, formally, when $(d, \varphi_1, \varphi_2) \in \mathscr{B}_{\varepsilon'}(d^0, \pi/2, -\pi/2)$, where $\mathscr{B}_{\varepsilon'}$ denotes an open ball of radius ε' centered at $(d^0, \pi/2, -\pi/2)$.

To study the input uncertainty rejection capability of the controller, we define Δ_{v_1}, Δ_{v_2}, Δ_{ω_1}, and Δ_{ω_2} to be the uncertainties on the velocity inputs. Assume that the $\mathscr{H}_\infty$ norms of all of the above are bounded from above, where we define the $\mathscr{H}_\infty$ norm of Δ_{v_1} (and hence all the other uncertainty terms) as $\|\Delta_{v_1}\|_\infty \triangleq \sup|\Delta_{v_1}|$. Looking at these uncertainties as virtual inputs, we can write:

$$\begin{bmatrix}\dot{\mathscr{D}}_d\\ \dot{\mathscr{D}}_1\\ \dot{\mathscr{D}}_2\end{bmatrix} = A\begin{bmatrix}\mathscr{D}_d\\ \mathscr{D}_1\\ \mathscr{D}_2\end{bmatrix} + B\begin{bmatrix}\Delta_{v_1}\\ \Delta_{v_2}\\ \Delta_{\omega_1}\\ \Delta_{\omega_2}\end{bmatrix}, \tag{9}$$

where

$$A = \begin{bmatrix}-k_d\frac{v_1+v_2+\Delta_{v_1}+\Delta_{v_2}}{2} & -v_1-\Delta_{v_1} & -v_2-\Delta_{v_2}\\ 0 & -k_{\mathscr{D}_1} & 0\\ 0 & 0 & -k_{\mathscr{D}_2}\end{bmatrix}, \tag{10a}$$

and

$$B = \begin{bmatrix}0 & \frac{-2\sin^2\varphi_1 + k_d d\cos\varphi_1}{2d} & \frac{-2\sin\varphi_1\sin\varphi_2 + k_d d\cos\varphi_1}{2d}\\ 0 & \frac{-2\sin\varphi_1\sin\varphi_2 + k_d d\cos\varphi_2}{2d} & \frac{-2\sin^2\varphi_2 + k_d d\cos\varphi_2}{2d}\\ 0 & -\sin\varphi_1 & 0\\ 0 & 0 & -\sin\varphi_2\end{bmatrix}^{\mathsf{T}}. \tag{10b}$$

We will now try to show that the system (9) is input-to-state stable with respect to the terms Δ_{v_1}, Δ_{v_2}, Δ_{ω_1}, and Δ_{ω_2}. The definition of input-to-state stability which we use is as follows:

Definition 1. The system $\dot{x} = f(t,x,u)$ is said to be input-to-state stable if there exist a class $\mathscr{KL}$ function β and a class $\mathscr{K}$ function γ such that for any initial state $x(t_0)$ and any bounded input $u(t)$, the solution $x(t)$ exists for all $t \geq t_0$ and satisfies $\|x(t)\| \leq \beta(\|x(t_0)\|, t-t_0) + \gamma\left(\sup_{t_0\leq\tau\leq t}\|u(\tau)\|\right)$. This definition of input-to-state stability is taken from Definition 4.7 in [24].

To prove input-to-state stability for (9), we use the following lemma:

Lemma 1 (Lemma 4.6 in [24])**.** *Suppose* $f(t,x,u)$ *is continuously differentiable and globally Lipschitz in* (x,u)*, uniformly in* t*. If the unforced system* $f(t,x,0)$ *has a globally exponentially stable equilibrium, then* $\dot{x} = f(t,x,u)$ *is input-to-state stable.*

We then have the following proposition:

Proposition 2. *The system* (9) *is input-to-state stable with respect to the disturbance uncertainties* Δ_{v_1}, Δ_{v_2}, Δ_{ω_1}, *and* Δ_{ω_2}.

Proof. The system (9) reduces to (8) when we consider no disturbance inputs. We have already shown that the system (8) has

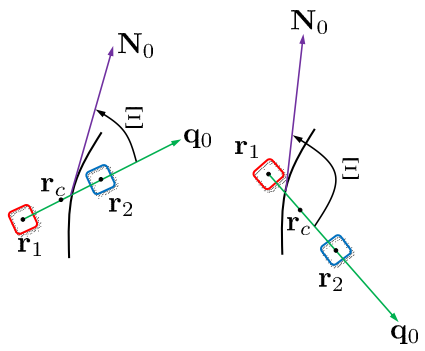

FIGURE 3. Summary of possible cases that may arise when the 2−agent unicycle formation is trying to track a level curve. Ξ denotes the angle between $\mathbf{N}_0$ and $\mathbf{q}_0$. Case 1 of the algorithm applies to the first figure, and case 4 applies to the second figure. As is clear from the figures, Ξ is acute in the Case 1 state and obtuse in the Case 4 state.

a globally exponentially stable equilibrium point. In addition, all the terms in A are continuously differentiable. The partial derivatives of the system (9) with respect to $\mathscr{D}_d, \mathscr{D}_1, \mathscr{D}_2, \Delta_{v_1}, \Delta_{v_2}, \Delta_{\omega_1}$, and Δ_{ω_2} are globally bounded uniformly with time, as $\Delta_{v_1}, \Delta_{v_2}$, Δ_{ω_1}, and Δ_{ω_2} are $\mathscr{H}_\infty$ bounded. This proves the globally Lipschitz property of (9), and therefore input-to-state stability follows immediately. ■

CURVE-TRACKING MODULE

The purpose of the curve-tracking module, as is clear from Fig. 1 is to take as input the noisy level values at the positions of the agents (denoted by $y(\mathbf{r}_1)$ and $y(\mathbf{r}_2)$) and use these two measurements to design the forward velocities v_1 and v_2 of the agents without estimating the field gradient. That the unicycle dynamics is controllable is a well-known result in the literature. For the sake of notational simplicity, the noisy measurements of the field by the sensors will henceforth be denoted by y_1 and y_2 instead of $y(\mathbf{r}_1)$ and $y(\mathbf{r}_2)$. Further, we define $y_c = (y_1 + y_2)/2$. Under Assumption 1, y_c gives us a satisfactory estimate of the level value at the formation center without having to install a third sensor.

Assuming that the two robots are already in formation, with $d = d^0$, $\varphi_1 = \pi/2$ and $\varphi_2 = -\pi/2$, in this section, we design v_1 and v_2 satisfying $v_1 + v_2 \geq 2v$ such that the moving direction of the formation center is first aligned with the tangent direction to the level curve and the formation center converges to and tracks the level curve having a desired level value z_d. We first design our hybrid (switched) control law to do the same, and then proceed to prove global asymptotic stability of our switched controller.

Design of the Control Law

We are given that the two mobile robots communicate and each one has access to the measurements and relative positions of the other robot. We propose the following simple hybrid control law:

$$v_1 - v_2 = \frac{v_{\max}}{2}\mathrm{sgn}(\dot{y}_c)\left(1 + \mathrm{sgn}(\dot{y}_c(y_c - z_d))\right), \tag{11}$$

where $\dot{y}_c = \frac{\mathrm{d}y_c}{\mathrm{d}t}$ and the signum function $\mathrm{sgn}(\cdot)$ is defined as follows:

$$\mathrm{sgn}(x) = \begin{cases} -1, & \text{if } x < 0, \\ 0, & \text{if } x = 0, \\ 1, & \text{if } x > 0. \end{cases}$$

The switched controller as written in the above concise form may be difficult to understand. To intuitively understand its working, we expand our control law on a case-by-case basis. This gives us the following detailed form of the controller:

1. If $\dot{y}_c > 0$ and $y_c - z_d > \varepsilon$

$$\begin{cases} v_1 = v_{\max}, \\ v_2 = 0. \end{cases} \tag{12a}$$

2. If $\dot{y}_c > 0$ and $y_c - z_d < -\varepsilon$

$$\begin{cases} v_1 = v_{\max}, \\ v_2 = v_{\max}. \end{cases} \tag{12b}$$

3. If $\dot{y}_c < 0$ and $y_c - z_d > \varepsilon$

$$\begin{cases} v_1 = v_{\max}, \\ v_2 = v_{\max}. \end{cases} \tag{12c}$$

4. If $\dot{y}_c < 0$ and $y_c - z_d < -\varepsilon$

$$\begin{cases} v_1 = 0, \\ v_2 = v_{\max}, \end{cases} \tag{12d}$$

where $\varepsilon \geq 0$ is an arbitrarily small positive quantity. The above equations essentially detail a hybrid controller with four switching modes, and form the basis of the curve-tracking module. The speeds v_1 and v_2 are taken from the set $\{0, v_{\max}\}$. A simple substitution of the cases of equation (12) into the equation (11)

shows that $(v_1 - v_2) = v_{\max}$ for case 1, $v_1 - v_2 = 0$ for cases 2 and 3, and $v_1 - v_2 = -v_{\max}$ for case 4, as required.
Physically, the working of the controller can be understood if we approximate the time derivative in the term $\dot{y}_c$ using a first-order Newton-Gregory backward difference formula. We then have $\dot{y}_c(t) \approx \frac{y_c(t)-y_c(t-1)}{t-(t-1)} = y_c(t) - y_c(t-1)$. The way the controller works is as follows: We use the difference between the field value at the formation center at any instant of time and the field value at the formation center at the previous instant of time, and the maximum velocity of the two robots to make them converge to the level curve and keep them moving along the same when convergence has been achieved. Both the robots are imparted a velocity of $v_{\max}$ either when heading towards the level curve or tracking it. If, at any point of time, the formation moves away from the level curve, only one of the robots is imparted a velocity of $v_{\max}$ to make the formation turn.

The four cases above can also be split into two modes, based on the behavior of the controller. Cases 2 and 3 define the 'seeking' mode, where the two-agent system first seeks the boundary of the desired level curve to be tracked. Cases 1 and 4 define the 'tracking' mode, where the two-agent system moves along the level curve, while tracking its perimeter.

The control law above describes behavior typical of hybrid control systems. The system dynamics is characterized by both continuous and discrete behavior, the former taking over when the system is in a particular mode, and the latter taking over when the system switches modes. To derive the dynamics of the system in each mode, define the unit vector pointing towards the direction of the tangent to the curve at the center of the formation as $\mathbf{N}_0$, and the unit normal and tangential vectors (with respect to the formation) at the formation center to be $\mathbf{n}_0 = \mathbf{n}_1 = \mathbf{n}_2$ and $\mathbf{q}_0 = \mathbf{q}_1 = -\mathbf{q}_2$ respectively. We also assume our state variables to be the field value at the formation center in the absence of noise, z_c, and the angle between $\mathbf{N}_0$ and $\mathbf{n}_0$, that is $\mathbf{N}_0^\mathsf{T}\mathbf{n}_0$. In the absence of noise, the dynamical equation for the field value at the formation center is given by $\dot{z}_c = \frac{\partial z_c}{\partial \mathbf{r}_c} \cdot \dot{\mathbf{r}}_c = \nabla z_c \cdot \mathbf{v}_c$.

Analysis of Stability and Convergence

In what follows, we will assume the complete absence of noisy measurements or corrupted field values. In other words, we assume $w(\mathbf{r}_i) \equiv 0$ in equation (3). This allows us to write z_c in place of y_c, and z_1, z_2 in place of y_1, y_2.

It is obvious that when formation control has been achieved, the speeds v_1 and v_2 are in the same direction. This means we can write the speed at the formation center as $v_c = (v_1 + v_2)/2$. We then introduce the following lemmas, required in proving the global asymptotic stability of our switched controller.

Lemma 2. *$\mathbf{N}_0^\mathsf{T}\mathbf{n}_0$ rises to a value greater than b, where $b \in (0,1)$, in finite time, and stays in the interval $(b,1]$ thereafter if the second-order spatial derivatives of the scalar field are sufficiently small compared to $\|\nabla z_c\|_2$. In other words, the moving direction of the formation is roughly aligned with the direction of the tangent to the level curve at the formation center.*

Proof. The way $\mathbf{N}_0$, $\mathbf{n}_0$, $\mathbf{n}_1$, $\mathbf{n}_2$, $\mathbf{q}_0$, $\mathbf{q}_1$, and $\mathbf{q}_2$ have been defined above allows us to write $\mathbf{N}_0 = -\dfrac{R_{\pi/2}\nabla z_c}{\|\nabla z_c\|_2}$, where $R_{\pi/2}$ is the matrix of 90° anticlockwise rotations, that is $R_{\pi/2} = \begin{bmatrix} 0 & -1 \\ 1 & 0 \end{bmatrix}$. We also have $\mathbf{q}_0 = \dfrac{\mathbf{r}_2 - \mathbf{r}_1}{d^0}$. We derive:

$$\dot{\mathbf{N}}_0^\mathsf{T}\mathbf{n}_0 = -\frac{v_1+v_2}{2\|\nabla z_c\|_2}\mathbf{n}_0^\mathsf{T}R_{\pi/2}^\mathsf{T}\begin{bmatrix} z_{xx} & z_{xy} \\ z_{xy} & z_{yy} \end{bmatrix}\Bigg|_{\mathbf{r}_c}\mathbf{n}_0 + \frac{v_1+v_2}{2\|\nabla z_c\|_2^3}\mathbf{n}_0^\mathsf{T}R_{\pi/2}^\mathsf{T}\begin{bmatrix} z_x^2 z_{xx} + z_x z_y z_{xy} & z_x^2 z_{xy} + z_x z_y z_{yy} \\ z_y^2 z_{xy} + z_x z_y z_{xx} & z_y^2 z_{yy} + z_x z_y z_{xy} \end{bmatrix}\Bigg|_{\mathbf{r}_c}\mathbf{n}_0, \quad (13)$$

and

$$\begin{aligned}\mathbf{N}_0^\mathsf{T}\dot{\mathbf{n}}_0 &= \left(\frac{v_1-v_2}{2}\right)\mathbf{N}_0^\mathsf{T}\mathbf{q}_0 \\ &= \left(\frac{v_1-v_2}{2}\right)\operatorname{sgn}(\mathbf{N}_0^\mathsf{T}\mathbf{q}_0)\sqrt{1-(\mathbf{N}_0^\mathsf{T}\mathbf{n}_0)^2}, \\ &= \left(\frac{v_1-v_2}{2}\right)\operatorname{sgn}\left(\frac{(\nabla z_c)^\mathsf{T}R_{\pi/2}^\mathsf{T}(\mathbf{r}_1-\mathbf{r}_2)}{d^0\|\nabla z_c\|_2}\right)\sqrt{1-(\mathbf{N}_0^\mathsf{T}\mathbf{n}_0)^2},\end{aligned} \quad (14)$$

where $z_x = \frac{\partial z}{\partial x}, z_y = \frac{\partial z}{\partial y}, z_{xx} = \frac{\partial^2 z}{\partial x^2}, z_{xy} = \frac{\partial^2 z}{\partial x \partial y}$, and $z_{yy} = \frac{\partial^2 z}{\partial y^2}$.

Next, consider the time-derivative of $\mathbf{N}_0^\mathsf{T}\mathbf{n}_0$:

$$\frac{\mathrm{d}(\mathbf{N}_0^\mathsf{T}\mathbf{n}_0)}{\mathrm{d}t} = \dot{\mathbf{N}}_0^\mathsf{T}\mathbf{n}_0 + \mathbf{N}_0^\mathsf{T}\dot{\mathbf{n}}_0. \quad (15)$$

The term $\dot{\mathbf{N}}_0^\mathsf{T}\mathbf{n}_0$ is sufficiently small since the second-order spatial derivatives of the scalar field are sufficiently small as compared to $\|\nabla z_c\|_2$, as already assumed. Let us now consider the term $\mathbf{N}_0^\mathsf{T}\dot{\mathbf{n}}_0$. There always exists $b \in (0,1)$ such that when $\mathbf{N}_0^\mathsf{T}\mathbf{n}_0 < b$, $|\mathbf{N}_0^\mathsf{T}\mathbf{q}_0| > \sqrt{1-b^2}$. Under the proposed control law, we also have $\frac{v_1-v_2}{2} = \frac{v_{\max}}{4}\operatorname{sgn}(\dot{z}_c)(1+\operatorname{sgn}(\dot{z}_c(z_c - z_d)))$, and $z_c \neq z_d$. Therefore, we have $\mathbf{N}_0^\mathsf{T}\dot{\mathbf{n}}_\mathbf{0} = \frac{v_{\max}}{4}\Upsilon\sqrt{1-(\mathbf{N}_0^\mathsf{T}\mathbf{n}_0)^2}$, where

$$\Upsilon = \operatorname{sgn}(\dot{z}_c)(1+\operatorname{sgn}(\dot{z}_c(z_c - z_d)))\operatorname{sgn}\left(\frac{(\nabla z_c)^\mathsf{T}R_{\pi/2}^\mathsf{T}(\mathbf{r}_1-\mathbf{r}_2)}{d^0\|\nabla z_c\|_2}\right). \quad (16)$$

Finding the value of Υ for cases 2 and 3 of the control law is relatively straightforward since for both these cases $\text{sgn}(\dot{z}_c)(1+\text{sgn}(\dot{z}_c(z_c-z_d)))=0$ and hence $\Upsilon=0$. The situation is a bit more involved for cases 1 and 4. We refer to Fig. 3 for the possible cases that can arise and focus on the numerator of the argument of the final signum function in equation (16). $((\nabla z_c)^\mathsf{T} R^\mathsf{T}_{\pi/2}(\mathbf{r}_1-\mathbf{r}_2))$ is just a scaling of the angle between the vectors $\mathbf{N}_0$ and $\mathbf{q}_0$. The angle between $\mathbf{N}_0$ and $\mathbf{q}_0$ (labeled Ξ in Fig. 3) is seen to be acute for case 1 and obtuse for case 4. This means that $\Upsilon=2$ for both cases 1 and 4. Therefore, $\frac{\mathrm{d}(\mathbf{N}_0^\mathsf{T}\mathbf{n}_0)}{\mathrm{d}t} \geq \frac{v_{\max}}{2}\sqrt{1-b^2}+\dot{\mathbf{N}}_0^\mathsf{T}\mathbf{n}_0$. The term $\dot{\mathbf{N}}_0^\mathsf{T}\mathbf{n}_0$ has already been assumed to be sufficiently small, and hence $\frac{\mathrm{d}(\mathbf{N}_0^\mathsf{T}\mathbf{n}_0)}{\mathrm{d}t}>0$. Therefore, $\mathbf{N}_0^\mathsf{T}\mathbf{n}_0$ rises above b and remains in the interval $(b,1]$ thereafter. ■

Next, following the approach used in [25], we define a function $h(z_c)$ satisfying the following assumptions, to be used in proving convergence of the level value at the formation center z_c to the desired level value z_d:

Assumption 3. 1. $h(z_c)$ is continuously differentiable on $(z_{\min}, z_{\max})$ and $f(z_c)=\frac{\mathrm{d}h}{\mathrm{d}z_c}$ is Lipschitz continuous.
2. $f(z_d)=0$ and $f(z)\neq 0$ if $z\neq z_d$.
3. $\lim\limits_{z\to z_{\min}} h(z) = \lim\limits_{z\to z_{\max}} h(z) = +\infty$. There also exists a $\tilde{z}$ such that $h(\tilde{z})=0$.

We then have the following lemma, which establishes global asymptotic stability for each of the four switched modes of our hybrid controller (12):

Lemma 3. *Define the closed (metric) annulus with $\varepsilon>0$ centered at a point z_d in a set M, $\mathscr{A}_\varepsilon[z_d]=\{z_c\in M \mid z_d-\varepsilon\leq d(z_c,z_d)\leq z_d+\varepsilon\}$ where the metric space (M,d) is any set M equipped with the ordinary Euclidean distance function d. Under the conditions of our discontinuous control law* (12) *and lemma 2, the moving direction of the formation is first roughly aligned with the direction of the tangent to the level curve at the formation center. Once this alignment has been achieved, the center of the formation converges globally to the level curve with the level value z_d asymptotically from the boundaries of the annulus $\mathscr{A}_\varepsilon[z_d]$.*

Proof. Since this is a switched (hybrid) system, we use different Lyapunov functions for the seeking and the tracking modes. We handle the former first, since it is easier to prove. Indeed, for the seeking mode (cases 2 and 3), convergence can be proved by considering the Lyapunov function $V_{\mathscr{S}}=\frac{1}{2}(z_c-z_d)^2$. $V_{\mathscr{S}}=0$ when $z_c=z_d$ and $V_{\mathscr{S}}>0$ when $z_c\neq z_d$. Also, $V_{\mathscr{S}}$ is polynomial, and hence continuously differentiable. The time-derivative of $V_{\mathscr{S}}$ along system trajectories is given by $\dot{V}_{\mathscr{S}}=(z_c-z_d)\dot{z}_c$. From cases 2 and 3, we have that when the $2-$agent formation is in the seeking mode, $\dot{z}_c$ and (z_c-z_d) are of the opposite sign. This gives $\dot{V}_{\mathscr{S}}<0$ and asymptotic stability of the equilibrium $z_c=z_d$ follows.

For the tracking mode (cases 1 and 4), we consider the Lyapunov function $V_{\mathscr{T}}=h(z_c)$, where $h(z_c)$ satisfies Assumptions 3. We then have $\dot{V}_{\mathscr{T}}=f(z_c)\dot{z}_c$. [25] gives an example of how to construct such a function f. Following a similar approach, we define $f(z_c)=\Gamma\left(\left(\frac{z_d}{z_c}\right)^2-1\right)$, where $\Gamma>0$ is a constant. The corresponding function $h(z_c)$ can be obtained by integrating $f(z_c)$. This yields $h(z_c)=\Gamma\int\left(\left(\frac{z_d}{z_c}\right)^2-1\right)\mathrm{d}z_c=-\Gamma\left(\frac{z_d^2}{z_c}+z_c\right)+C$, where C is the constant of integration. Since there exists a $\tilde{z}\in[z_{\min},z_{\max}]$ such that $h(\tilde{z})=0$ according to Assumption 3, we have $-\Gamma\left(\frac{z_d^2}{\tilde{z}}+\tilde{z}\right)+C=0$, and, $h(z_c)=-\Gamma\left(\frac{z_d^2}{z_c}+z_c\right)+\Gamma\left(\frac{z_d^2}{\tilde{z}}+\tilde{z}\right)$. In the tracking mode, $\dot{z}_c$ and (z_c-z_d) are of the same sign. For case 1, $(z_c-z_d)>0$. This means that $f(z_c)<0$ and $\dot{V}_{\mathscr{T}}=f(z_c)\dot{z}_c<0$ since $\dot{z}_c>0$. For case 4, $(z_c-z_d)<0$. This means that $f(z_c)>0$ and $\dot{V}_{\mathscr{T}}=f(z_c)\dot{z}_c<0$ since $\dot{z}_c<0$. Hence, the field value at the formation center converges asymptotically to the desired value z_d. It is also interesting to note here that both the Lyapunov functions $V_{\mathscr{S}}$ and $V_{\mathscr{T}}$, defined above, are radially unbounded and therefore the equilibrium $z_c=z_d$ is globally asymptotically stable in both cases. ■

Now that stability has been established for each of the four switched modes of the system, we proceed to prove global asymptotic stability for the composite switched system. To do that, we need the following lemma, introduced as follows:

Lemma 4 (Theorem 3.1 in [26])**.** *Suppose that we are given a family f_p, $p\in\mathfrak{P}$, of (at least) locally Lipschitz functions from $\mathbb{R}^n$ to $\mathbb{R}^n$, where $\mathfrak{P}=\{1,2,\cdots,m\}$ is some finite index set (typically a subset of a finite-dimensional linear vector space), and where f_p gives rise to a family of globally asymptotically stable systems $\dot{x}=f_p(x)$, $p\in\mathfrak{P}$, evolving on $\mathbb{R}^n$, and a piecewise constant switching function $\sigma:[0,\infty)\to\mathfrak{P}$. σ specifies at each time instant t, the index $\sigma(t)\in\mathfrak{P}$ of the active subsystem. Also, let $V_p, p\in\mathfrak{P}$ be a family of corresponding radially unbounded Lyapunov functions. Suppose that there exists a family of positive definite continuous functions $W_p, p\in\mathfrak{P}$ with the property that for every pair of switching times (t_i,t_j), $i<j$ such that $\sigma(t_i)=\sigma(t_j)=p\in\mathfrak{P}$ and $\sigma(t_k)\neq p$ for $t_i<t_k<t_j$, we have $V_p(x(t_j))-V_p(x(t_i))\leq -W_p(x(t_i))$. Then the switched system $\dot{x}(t)=f_{\sigma(t)}(x(t))$ is globally asymptotically stable.*

We are now ready to state and prove our main result:

Theorem 1. *The hybrid controller defined in* (12) *is globally asymptotically stable.*

Proof. We use the idea of lemma 4 in our proof. To prove this theorem, we essentially need to show that both our Lyapunov

functions $V_{\mathscr{S}}$ and $V_{\mathscr{T}}$ form a decreasing sequence for every possible pair of switching times, that is, $(V_{\mathscr{S}}(z_c(t_j)) - V_{\mathscr{S}}(z_c(t_i))) \leq -W_1(z_c(t_i))$ and $(V_{\mathscr{T}}(z_c(t_j)) - V_{\mathscr{T}}(z_c(t_i))) \leq -W_2(z_c(t_i))$ for possible every pair of switching times (t_i, t_j), $i < j$, for positive definite continuous functions W_1 and W_2.

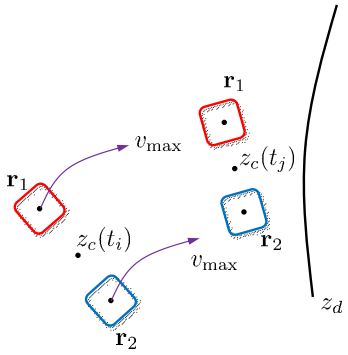

FIGURE 4. One possible motion of the two mobile robots when they are in the seeking mode. Note that for any possible pair of switching times (t_i, t_j), $i < j$, we have $|z_c(t_j) - z_d| < |z_c(t_i) - z_d|$. The level curve is shown in black.

Consider the difference

$$V_{\mathscr{S}}(z_c(t_j)) - V_{\mathscr{S}}(z_c(t_i)) = \frac{1}{2}(z_c(t_j) - z_d)^2 - \frac{1}{2}(z_c(t_i) - z_d)^2, \tag{17}$$
$$= \frac{1}{2}(d_{j,z_d}^2 - d_{i,z_d}^2).$$

where $d_{j,z_d} = |z_c(t_j) - z_d|$, $d_{i,z_d} = |z_c(t_i) - z_d|$. We introduce the absolute value of the difference between the level value at the formation center and the desired level value because the formation center can seek the level curve from both inside and outside its boundary. As is clear from Fig. 4, under the assumptions of our control law, we find that in the seeking mode (case 2 or case 3), the two-agent system first seeks the boundary of the level curve that is desired to be tracked. This means that for any $i < j$, $d_{j,z_d} \leq d_{i,z_d}$, since the formation center continually moves towards the level curve. So we conclude that $V_{\mathscr{S}}(z_c(t_j)) - V_{\mathscr{S}}(z_c(t_i)) \leq 0$, and the sequence $\{V_{\mathscr{S}}(z_c(t_n))\}_{n=1}^{\infty}$ is a decreasing sequence. Also, for $\Gamma > 0$, $z_c(t_i), z_c(t_j), z_d > 0$, we have that the difference $V_{\mathscr{T}}(z_c(t_j)) - V_{\mathscr{T}}(z_c(t_i)) \leq 0$. The above inequality can be simplified to $\frac{z_d^2 z_c(t_i) - z_d^2 z_c(t_j) + z_c(t_i) z_c^2(t_j) - z_c^2(t_i) z_c(t_j)}{z_c(t_i) z_c(t_j)} \geq 0$, which is equivalent to saying that $-z_d^2(z_c(t_j) - z_c(t_i)) + z_c(t_i) z_c(t_j)(z_c(t_j) - z_c(t_i)) \geq 0$, or that $(z_c(t_j) - z_c(t_i))(z_c(t_i) z_c(t_j) - z_d^2) \geq 0$ which is true if

$$(z_c(t_j) - z_c(t_i))(z_d^2 - z_c(t_i) z_c(t_j)) \leq 0. \tag{18}$$

Now, for every pair of switching times (t_i, t_j), $i < j$, for case 1 of the tracking mode, we have $\dot{z}_c \geq 0$ from the control law, which implies that $(z_c(t_j) - z_c(t_i)) \geq 0$, or $z_c(t_j) \geq z_c(t_i)$. Multiplying both sides of this inequality by $z_c(t_i)$ (which is positive, and preserves the sign of the inequality) gives us $z_c(t_i) z_c(t_j) \geq z_c^2(t_i)$. Also, from the control law in case 1, we have $z_c - z_d \geq \varepsilon \geq 0$. So we can write $z_c(t_i) z_c(t_j) \geq z_c^2(t_i) \geq z_d^2$. So $z_d^2 \leq z_c(t_i) z_c(t_j)$, as required by (18). Similarly for case 4 of the tracking mode, we have $\dot{z}_c \leq 0$ which implies that $(z_c(t_j) - z_c(t_i)) \leq 0$, or $z_c(t_j) \leq z_c(t_i)$. Multiplying both sides of this inequality by $z_c(t_i)$ (which is positive, and preserves the sign of the inequality) gives us $z_c(t_i) z_c(t_j) \leq z_c^2(t_i)$. Also, from the control law in case 4, we have $z_c - z_d \leq -\varepsilon \leq 0$. Hence, $z_c(t_i) z_c(t_j) \leq z_c^2(t_i) \leq z_d^2$. So $z_d^2 \geq z_c(t_i) z_c(t_j)$, again, as required by (18). Thus, $V_{\mathscr{T}}(z_c(t_j)) - V_{\mathscr{T}}(z_c(t_i)) \leq 0$, and the sequence $\{V_{\mathscr{T}}(z_c(t_n))\}_{n=1}^{\infty}$ is a decreasing sequence. This completes the proof, and our switched controller is globally asymptotically stable. ■

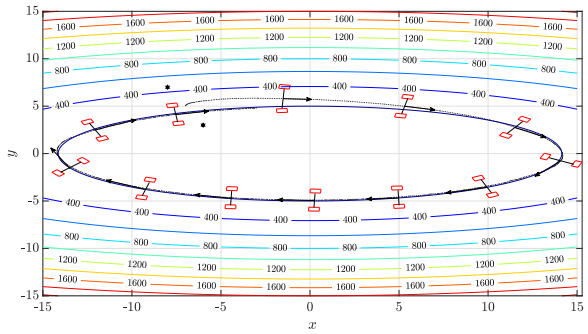

FIGURE 5. Motion of the 2−agent unicycle system for tracking noisy level curves with $z_d = 200$ for the scalar field $f_1(x,y) = x^2 + 8y^2$. The asterisks denote the initial starting positions of the two unicycles.

SIMULATION RESULTS

The performance of our control algorithm is tested first on an ellipse (which has degree two), and then on an algebraic curve having degree four.

Figures 5 and 6 show the performance of our algorithm on noisy level curves of the ellipse $z = f_1(x,y) = x^2 + 8y^2$. We track level curves having a desired level value $z_d = 200$. In Fig. 5, the red rectangles denote the two unicycles, the black asterisks denote the starting point for the two unicycles in the plane, and the black dots denote the position of the formation center as it evolves with each time step. Noise has been incorporated into the simulation by adding normally distributed random

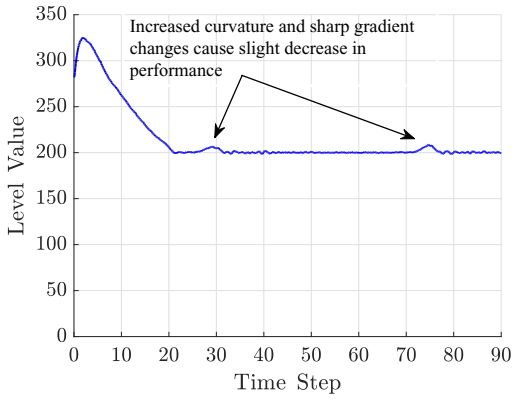

FIGURE 6. Evolution of tracked level value at the formation center with time for a 2−agent unicycle system tracking noisy level curves with $z_d = 200$ for the scalar field $f_1(x,y) = x^2 + 8y^2$.

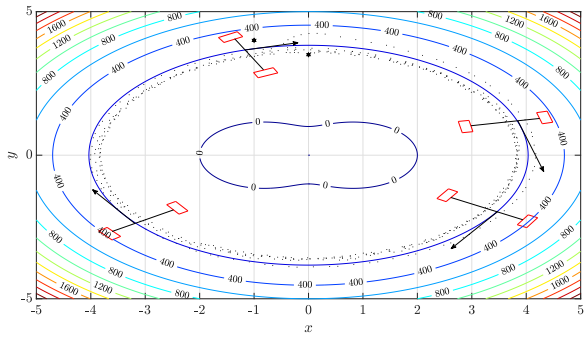

FIGURE 7. Motion of the 2−agent unicycle system for tracking noisy level curves with $z_d = 200$ for the scalar field $f_2(x,y) = (x^2+y^2)^2 - 4x^2 - y^2$. The asterisks denote the initial starting positions of the two unicycles.

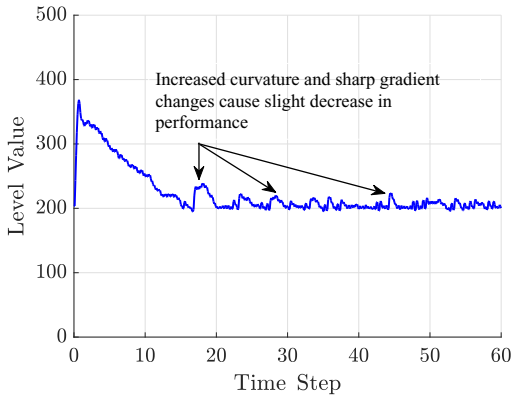

FIGURE 8. Evolution of tracked level value at the formation center with time for a 2−agent unicycle system tracking noisy level curves with $z_d = 200$ for the scalar field $f_2(x,y) = (x^2+y^2)^2 - 4x^2 - y^2$.

numbers drawn from the standard normal distribution $\mathcal{N}(0,1)$ to each field value. We use the following values for the constants: $d^0 = 2, v_{\max} = 1, k_d = k_{\mathscr{D}_1} = k_{\mathscr{D}_2} = 0.5$, and $\varepsilon = 10^{-4}$. The 2−agent unicycle system converges quickly and smoothly to the vicinity of the desired level curve, and its formation center tracks it with a high degree of accuracy with evolving time. In Fig. 6, the level value at the formation center is tracked as a function of time for the same system.

Our control algorithm is also tested on noisy level curves of the function $z = f_2(x,y) = (x^2+y^2)^2 - 4x^2 - y^2$. This is a rational algebraic curve of degree four, and is known in the literature as a hippopede [27]. Figures 7 and 8 show the performance of our control algorithm when used to track level curves of the hippopede having a desired level value $z_d = 200$. We use $d^0 = 2, v_{\max} = 3, k_d = k_{\mathscr{D}_1} = k_{\mathscr{D}_2} = 0.5$, and $\varepsilon = 10^{-10}$. Once again, we use additive noise in the form of normally distributed random numbers drawn from $\mathcal{N}(0,1)$. The 2−agent unicycle system takes slightly more time to converge to the vicinity of the level curve, owing to the more complicated landscape. Once convergence has been achieved, the system tracks the desired level curve with a high degree of accuracy. Fig. 8 shows the evolution of the level value at the formation center with time. We also note that in both the simulations, increased curvature and sharp changes in the field gradient cause a decrease of performance. Adaptive control of the algorithm parameters is a potential solution to this problem.

Our algorithm thus shows a relatively good performance on a wide class of noisy two-dimensional functions. The uniqueness of the work lies in the fact that the algorithm can track noisy level curves of many types of two-dimensional functions using two unicycles, without having to estimate the gradient of the field in question and using minimum computational power.

CONCLUSION

In this paper, we propose a gradient-free modular approach to the tracking of level curves in noisy scalar fields using two unicycles. We propose a dual control-module structure, in essence decoupling the design of the linear and angular velocities of the unicycles. While the formation control module deals with designing the angular velocities so that the unicycles maintain a constant separation at equilibrium, the curve tracking module deals with using the instantaneous noisy field values to design the forward linear velocities so that the system can quickly converge to the desired level curve and keep tracking it with time. Control-theoretic convergence results are then shown for both the modules. The algorithm demonstrates fast convergence and highly accurate tracking on many types of level curves. Possible future research directions include designing an adaptive control scheme for the constant parameters and generalizing the controller so that N unicycles can track a desired noisy level curve without explicit gradient estimation.

REFERENCES

[1] Sayyed, A., and Becker, L. B., 2015. *A Survey on Data Collection in Mobile Wireless Sensor Networks (MWSNs)*. Springer International Publishing, Cham, pp. 257–278.

[2] Amundson, I., and Koutsoukos, X. D., 2009. *A Survey on Localization for Mobile Wireless Sensor Networks*. Springer Berlin Heidelberg, Berlin, Heidelberg, pp. 235–254.

[3] Wang, Y., and Hussein, I. I., 2010. "Awareness coverage control over large-scale domains with intermittent communications". *IEEE Transactions on Automatic Control,* **55**(8), Aug, pp. 1850–1859.

[4] Zhu, C., Shu, L., Hara, T., Wang, L., and Nishio, S., 2010. "Research issues on mobile sensor networks". In Proceedings of the 2010 International ICST Conference on Communications and Networking in China (CHINACOM), pp. 1–6.

[5] Clark, J., and Fierro, R., 2005. "Cooperative hybrid control of robotic sensors for perimeter detection and tracking". In Proceedings of the 2005 American Control Conference, IEEE, pp. 3500–3505.

[6] Clark, J., and Fierro, R., 2007. "Mobile robotic sensors for perimeter detection and tracking". *ISA Transactions,* **46**(1), pp. 3 – 13.

[7] Hsieh, C. H., Jin, Z., Marthaler, D., Nguyen, B. Q., Tung, D. J., Bertozzi, A. L., and Murray, R. M., 2005. "Experimental validation of an algorithm for cooperative boundary tracking". In Proceedings of the 2005 American Control Conference, pp. 1078–1083 vol. 2.

[8] Joshi, A., Ashley, T., Huang, Y. R., and Bertozzi, A. L., 2009. "Experimental validation of cooperative environmental boundary tracking with on-board sensors". In Proceedings of the 2009 American Control Conference, pp. 2630–2635.

[9] Zhang, F., Fiorelli, E., and Leonard, N., 2007. "Exploring scalar fields using multiple sensor platforms: Tracking level curves". In Proceedings of the 2007 IEEE Conference on Decision and Control, pp. 3579–3584.

[10] Wu, W., and Zhang, F., 2011. "Cooperative exploration of level surfaces of three dimensional scalar fields". *Automatica,* **47**(9), pp. 2044 – 2051.

[11] Taubin, G., 1995. "Estimating the tensor of curvature of a surface from a polyhedral approximation". In Proceedings of the 1995 Internation Conference on Computer Vision, pp. 902–907.

[12] Barat, C., and Rendas, M. J., 2003. "Benthic boundary tracking using a profiler sonar". In Proceedings of the 2003 IEEE/RSJ International Conference on Intelligent Robots and Systems (IROS), Vol. 1, pp. 830–835.

[13] Kemp, M., Bertozzi, A. L., and Marthaler, D., 2004. "Multi-uuv perimeter surveillance". In Autonomous Underwater Vehicles, 2004 IEEE/OES, pp. 102–107.

[14] Andersson, S. B., 2007. "Curve tracking for rapid imaging in afm". *IEEE Transactions on NanoBioscience,* **6**(4), Dec, pp. 354–361.

[15] Matveev, A. S., Teimoori, H., and Savkin, A. V., 2012. "Method for tracking of environmental level sets by a unicycle-like vehicle". *Automatica,* **48**(9), pp. 2252 – 2261.

[16] Menon, P. P., Edwards, C., Shtessel, Y. B., Ghose, D., and Haywood, J., 2014. "Boundary tracking using a suboptimal sliding mode algorithm". In Proceedings of the 2014 IEEE Conference on Decision and Control, pp. 5518–5523.

[17] Matveev, A. S., Hoy, M. C., Ovchinnikov, K., Anisimov, A., and Savkin, A. V., 2015. "Robot navigation for monitoring unsteady environmental boundaries without field gradient estimation". *Automatica,* **62**, pp. 227 – 235.

[18] Matveev, A. S., Semakova, A. A., and Savkin, A. V., 2016. "Environmental boundary tracking approach to close circumnavigation of a group of unknown moving targets using range measurements". In Proceedings of the 2016 Chinese Control Conference, pp. 5492–5497.

[19] Qin, X., He, S., Quintero, C. P., Singh, A., Dehghan, M., and Jagersand, M., 2017. "Real-time salient closed boundary tracking via line segments perceptual grouping". In Proceedings of the 2017 IEEE/RSJ International Conference on Intelligent Robots and Systems (IROS), pp. 4284–4289.

[20] Mellucci, C., Menon, P. P., Edwards, C., and Challenor, P., 2017. "Experimental validation of boundary tracking using the suboptimal sliding mode algorithm". In Proceedings of the 2017 American Control Conference, pp. 4878–4883.

[21] Chatterjee, S., and Wu, W., 2017. "Cooperative curve tracking in two dimensions without explicit estimation of the field gradient". In Proceedings of the 2017 4th International Conference on Control, Decision and Information Technologies (CoDIT), pp. 0167–0172.

[22] Lu, L., You, J., and Wu, W., 2016. "Constrained fast source seeking using two nonholonomic mobile robots". In Proceedings of the 2016 American Control Conference, pp. 7295–7301.

[23] Kühnel, W., 2002. *Differential Geometry*. American Mathematical Society.

[24] Khalil, H. K., 2002. *Nonlinear Systems*, 3rd ed. Prentice-Hall, Englewood Cliffs, NJ.

[25] Justh, E. W., and Krishnaprasad, P. S., 2005. "Natural frames and interacting particles in three dimensions". In Proceedings of the 2005 IEEE Conference on Decision and Control, pp. 2841–2846.

[26] Liberzon, D., 2003. "Switching in systems and control, ser. systems & control: Foundations & applications". *Birkhauser*.

[27] Lawrence, J. D., 2013. *A catalog of special plane curves*. Courier Corporation.